Measurements and calculations of metastable level lifetimes in Fe X, Fe XI, Fe XII, Fe XIII, and Fe XIV

D. P. Moehs,[1,*] M. I. Bhatti,[2] and D. A. Church[1]

[1]*Physics Department, Texas A&M University, College Station, Texas 77843-4242*
[2]*Physics and Geology Department, University of Texas Pan American, Edinburg, Texas 78539*

Lifetimes of metastable levels in the ground term of Fe ions within the $3s^2 3p^k$, $k = 1-5$, isoelectronic sequences have been measured. These measurements were performed utilizing ions that were selected by mass to charge ratio while transported from an electron cyclotron resonance ion source to a Kingdon ion trap, where they were captured and then confined for periods of up to 2.1 s. During this storage period, selected emission wavelengths of transitions from metastable levels in the visible or near-ultraviolet spectral regions were isolated using interference filters, and the time-dependent fluorescence intensities were measured using a photomultiplier tube. Measurement precisions on the order of 2% were achieved in favorable cases. The measured lifetimes are τ(Fe X, $3s^2 3p^5\ {}^2P_{1/2}) = 13.64 \pm 0.25$ ms, τ(Fe XI, $3s^2 3p^4\ {}^1D_2) = 9.86 \pm 0.22$ ms, τ(Fe XII, $3s^2 3p^3\ {}^2P_{3/2}) = 1.85 \pm 0.24$ ms, τ(Fe XII, $3s^2 3p^3\ {}^2P_{1/2}) = 4.38 \pm 0.42$ ms, τ(Fe XII, $3s^2 3p^3\ {}^2D_{3/2}) = 20.35 \pm 1.24$ ms, τ(Fe XIII, $3s^2 3p^2\ {}^1D_2) = 6.93 \pm 0.18$ ms, and τ(Fe XIV, $3s^2 3p\ {}^2P_{3/2}) = 17.52 \pm 0.29$ ms. These results are compared with existing and with new theoretical calculations, which have estimated uncertainties on the order of 10–25 %.

I. INTRODUCTION

Iron is an important and pervasive astrophysical element, due to the significance of its nuclear binding energy to stellar evolution and to the synthesis of the elements. Forbidden transitions of the ions of Fe are consequently prominent in the solar corona, such as the well-known ''red'' and ''green'' coronal transitions, occurring in Fe X and Fe XIV respectively, which are commonly observed in other astrophysical environments as well. Lifetimes of these and similar forbidden transitions are important to certain remote plasma diagnostics [1]. Consequently the energies and transition rates of metastable levels in the ground and excited terms of Fe ions have been frequently calculated. Measurements of the lifetimes of ground term metastable levels of ions with low charge using traps [2] have continued since the technique was originated in the 1970s [3]. However, laboratory lifetime measurements for long-lived levels of more highly charged ions, to test these calculations, have become possible only relatively recently [4–6]. The innovations responsible for the present measurements include (1) the development of the electron cyclotron resonance ion source [7], which can provide a stable source of multiply charged metal ion beams; and (2) the capture of these ions, following charge-to-mass selection, into a Kingdon ion trap [8,9], where they are stably confined under ultrahigh-vacuum conditions.

The present measurements were completed on transitions between ground term levels of Fe X through Fe XIV, which have wavelengths in the visible or ultraviolet spectral regions, and which have lifetimes ≥ 2 ms. Due to the λ^{-3}

dependence of magnetic dipole ($M1$) transition rates, these conditions tend to be related. The lower limit of the lifetime measurements is set by ion settling in the trap following capture, while the upper limit is set by ion-neutral collisions resulting in a change in charge due to electron capture [10].

Experimental wavelengths are available for many forbidden transitions of Fe ions [11], so the present lifetime measurements provide some data to test whether the accuracy (currently 10–50%) of theoretical transition rate calculations is limited by the accuracies of the calculated wavelengths, or of the matrix elements. This was not feasible for earlier measurements on ions of Mn [12]. *Ab initio* theoretical transition rate calculations based on relativistic configuration interaction theory, including low-order QED corrections, are found to be improved when experimental wavelengths are used, but still differed from experiment by 2–3 standard deviations of the experimental error.

II. APPARATUS AND TECHNIQUE

The electrostatic Kingdon trap used to confine ions for these measurements, and the operation of the electron cyclotron resonance (ECR) ion source used to produce the metastable Fe ions, have been thoroughly documented in a recent publication [9], which should be consulted for details and technique. Multiply charged Fe ions were produced in the ECR ion source when Fe metal was evaporated from an axially inserted thermal oven into the source region. Oxygen was used to support the ECR plasma, except for a beam of Fe^{11+} where nitrogen was used to optimize output. Stable beams of Fe^{q+} ($5 < q < 13$) with electrical currents between 1.4–0.5 μA were produced in this manner. A pulsed (100 μs) beam of Fe ions, with a charge-to-mass ratio selected using a 90° bending magnet, was electrostatically focused, deflected, and decelerated prior to entering the midplane of the Kingdon trap, where ions were captured by pulsing the

*Physics Division, Bldg. 203, Argonne National Laboratory, Argonne, IL 60439.

TABLE I. New calculations using the B-spline basis set with the modified GRASP2 code, including Breit and QED corrections, of particular lifetimes and energy-level separations. These are compared with measured values.

Ion	Transition	Energy-level separations (a.u.)		Lifetime (ms)		Measured lifetime (ms)
		Expt.	Theory	*ab initio*	semiemp.	
Fe X $(3p^5)$	$^2P_{3/2}-^2P_{1/2}$	-0.07147	-0.07128	14.54	14.42	13.64 ± 0.25
Fe XI $(3p^4)$	$^3P_2-^1D_2$	-0.17202	-0.17078			
				10.8	10.65	9.86 ± 0.22
	$^3P_1-^1D_2$	-0.11428	-0.11643			
Fe XII $(3p^3)$	$^4S_{1/2}-^2D_{3/2}$	-0.18939	-0.21152	16.29	22.57	20.35 ± 1.24
Fe XIII $(3p^2)$	$^3P_2-^1D_2$	-0.13448	-0.14172			
				6.26	7.23	6.93 ± 0.18
	$^3P_1-^1D_2$	-0.17669	-0.18434			
Fe XIV $(3p)$	$^2P_{1/2}-^2P_{3/2}$	-0.08517	-0.08592	17.01	16.57	17.52 ± 0.29

central wire. Fe ion storage time constants in the Kingdon trap were typically >1.5 s for these measurements, at pressures near 5×10^{-10} Torr. The detected photon count from the metastable decays consistently showed an initial fast transient with a time constant of 1.2 ± 0.3 ms, thought to be associated with ion settling in the trap following capture. This transient, plus the slower signal changes associated with the metastable level decays, were fitted to two exponentials plus a constant background. In some analyses, the data points associated with the transient were removed from the fit.

III. THEORY

New calculations of rates and energy-level separations for many of the levels presently studied have been completed using a relativistic multiconfiguration method based on a complete set of discrete B-spline orbitals. These orbitals were solutions of the radial Dirac equation for an electron moving in a central potential, but confined to a cavity with a finite radius [13]. Atomic state functions were constructed for the desired state by taking a known linear combination of configuration state functions from the B-spline single-particle orbitals, chosen to have the same total angular momentum and parity. The contribution to the matrix elements from the Coulomb Hamiltonian were coupled with the first-order Breit interaction [14], and with the Lamb shift in lowest order. A configuration interaction matrix as large as 2025 relativistic configurations, based on a much smaller number of nonrelativistic configurations, was diagonalized by applying the variational principle to the energy functional with respect to the mixing coefficients, subject to the wave-function normalization condition. This leads to the configuration interaction equation, which determines the mixing coefficients and the corrected energy levels. The major contributions to the atomic $M1$ transitions came from nearby states with the same parity. Correlation effects were included by adding odd configuration state functions. Since the energy

separations were calculated, the transition rate results could be compared with adjusted rates using experimental wavelengths. Employment of the experimental energy separations in the transition rate calculation constitutes a semiempirical approximation, which has been tested as well. The experimental and theoretical energy-level separations and the *ab initio* and semiempirical lifetimes appear in Table I, along with the experimental lifetimes and uncertainties.

Because of the astrophysical significance of Fe ions, particularly in solar physics, the transition rates presented in this work were previously calculated a number of times with different theoretical models using varying degrees of approximation. Eidelsberg, Crifo-Magnant, and Zeippen [15] were among the first to tabulate transition rates for forbidden lines observed in astronomical sources. The calculations were taken from the literature prior to 1981, or extrapolated along isoelectronic sequences. All of the experimental lifetimes presented in this work were included. Subsequently Mendoza and Zeippen calculated the transition rates within the $3s^23p^2$ [16], $3s^23p^3$ [17], and $3s^23p^4$ [18] configurations of Fe ions, using a scaled Thomas-Fermi model. During this same time period, Huang and co-workers calculated energy levels and transition rates for Fe X [19], XI [20], XII [21], XIII [22], and XIV [23] using the multiconfiguration Dirac-Fock (MCDF) method. Kaufman and Sugar [13], as well as Fuhr, Martin, and Wiese [11], tabulated these and other calculations. More recent theoretical work for Fe X [24] and Fe XI [25] by Bhatia and Doschek used configuration-interaction wave functions, with each configuration an expansion in terms of Slater states built from Slater orbitals. Results of the previous calculations pertinent to the present measurements appear in Table II.

IV. MEASUREMENTS

A. Fe x, $3s^23p^5\,^2P_{1/2}$

The ground term of Fe X is a two-level system with the upper $^2P_{1/2}$ level decaying through a magnetic dipole ($M1$)

TABLE II. Previously calculated lifetimes of levels of Fe X–Fe XIV ions pertinent to the present measurements. Many of these lifetimes are plotted in Fig. 6. References and lifetimes for related Mn IX–XIII ion levels plotted in Fig. 6 can be found in Ref. [12].

Ion	Level	Theoretical lifetime (ms)	Reference
Fe X	$3s^2 3p^5\ {}^2P_{1/2}$	18.20	[24]
		16.59	[19]
		14.44	[11,13]
		14.37	[15]
		13.64(25)	present expt.
Fe XI	$3s^2 3p^4\ {}^1D_2$	10.55	[15]
		9.99	[20]
		9.84	[11,18]
		9.83	[13]
		9.81	[25]
		9.86(22)	present expt.
Fe XII	$3s^2 3p^3\ {}^2P_{3/2}$	1.67	[11,13,21]
		1.64	[15]
		1.55	[17]
		1.85(24)	present expt.
	$3s^2 3p^3\ {}^2P_{1/2}$	4.08	[11]
		3.98	[13,21]
		3.84	[15]
		3.63	[17]
		4.38(42)	present expt.
	$3s^2 3p^3\ {}^2D_{3/2}$	20.79	[11,13,21]
		18.87	[15]
		16.20	[17]
		20.35(1.24)	present expt.
Fe XIII	$3s^2 3p^2\ {}^1D_2$	9.69	[13]
		7.24	[11,22]
		6.45	[16]
		6.29	[15]
		6.93(18)	present expt.
Fe XIV	$3s^2 3p\ {}^2P_{1/2}$	16.63	[11,13,15,23]
		17.52(29)	present expt.

transition to the $^2P_{3/2}$ level at the well-known "red line" wavelength of 637.5 nm. Based on the multiplicity of the two levels, the population of the upper level is estimated to be around 33%. Slow transitions between highly excited metastable levels above the ground term were also observed [26], suggesting that the initial populations may be somewhat smaller than the above estimate. These upper levels are known to predominantly cascade into the $^2P_{3/2}$ level via $M1$ transitions, and do not effect the measured $^2P_{1/2}$ lifetime [11]. A cooled red-sensitive photomultiplier tube with a quantum efficiency near 5% was used to collect the data, which appears in Ref. [27]. The lifetime τ(Fe X, $3s^2 3p^5\ ^2P_{1/2}$)$=13.64\pm0.25$ ms, with a final precision of 1.8%, was determined. It agrees best with the earlier calculations tabulated by Eidelsberg, Crifo-Magnant, and Zeippen [15] and Kaufman and Sugar [13]; see Table II.

B. Fe XI, $3s^2 3p^4\ ^1D_2$

The dominant $M1$ transitions within the ground term of Fe XI and their associated theoretical transition rates [11] are

shown in Fig. 1. Assuming a statistical weight for the population of the sublevels within the ground term, approximately 33% of the stored ions should be in the $^1D_2$ level. The contribution to this population from the rapidly cascading $^1S_0$ level is expected to be insignificant due to the very small branching ratio ($\leq1\%$) and relatively small upper-level population. The $^1D_2$ level decays predominantly through
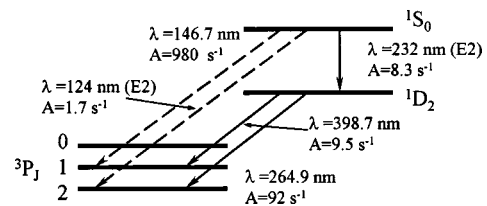

FIG. 1. The ground term level diagram for Fe XI, with transition rates and wavelengths from Fuhr, Martin, and Wiese [11]. Unlabeled decay paths are predominantly associated with $M1$ transitions.
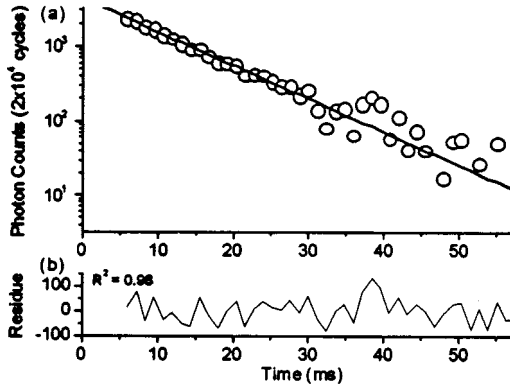
FIG. 2. Photon count data for the Fe XI $^3P_2$-$^1D_2$ transition at 264.9 nm, with the background subtracted, fitted by a single exponential. The residue of the fit is also shown. Initial data points representing a rapid signal transient were removed prior to the fit, which yielded a decay time constant of 9.81 ± 0.21 ms.

two $M1$ transitions to the $^3P_2$ and $^3P_1$ levels. Observation of this level decay was made using the first of these transitions having a branching ratio of 91%. A beam current of 0.8 μA of Fe^{10+} ions obtained from the ion source resulted in roughly 5.0×10^5 stored ions per cycle. The logarithm of the photon count data set including data from 2×10^4 trapping cycles is plotted as a function of time in Fig. 2, together with the residuals of the fit. The first few data points, corresponding to an initial ion transient, and the background, were removed prior to fitting, and the remaining data were fitted with a single exponential. The resulting decay constant was $\tau_m = 9.81 \pm 0.21$ ms. Correcting for the finite ion storage time, a level lifetime of $\tau(Fe\ XI, 3s^2 3p^4\ ^1D_2) = 9.86 \pm 0.22$ ms is obtained. The only calculation not within one standard deviation of the measurement is that tabulated in Ref. [15].

C. Fe XII, $3s^2 3p^3\ ^2P_{3/2}$, $^2P_{1/2}$, and $^2D_{3/2}$

The level diagram for the ground term of Fe XII appears in Fig. 3. Fe^{11+} beam currents of 0.78 and 0.52 μA were ob-
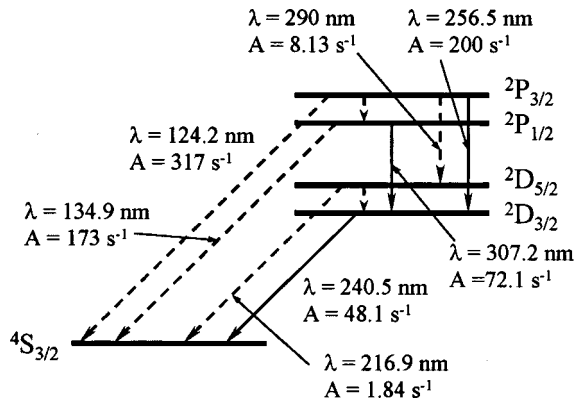

FIG. 3. The ground term level diagram for Fe XII, showing the theoretical rates and wavelengths of the primary decay modes [11]. All of the decay paths shown are predominantly associated with $M1$ transitions.
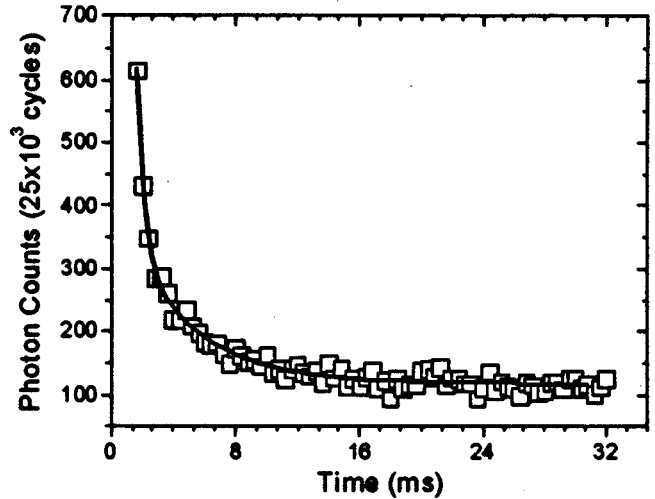

FIG. 4. Plot showing data for the first direct observation of the Fe XII $^2D_{3/2}$-$^2P_{1/2}$ transition near 307 nm. The photon count data were fitted by a double exponential and constant background, resulting in a decay time constant of 4.37 ± 0.42 ms.

tained on two consecutive days. The stronger of the two currents resulted in roughly 5×10^5 stored ions.

The $^2P_{3/2}$ level decays principally through four $M1$ transitions. Isolation of the $^2D_{3/2}$-$^2P_{3/2}$ decay at 256.5 nm was achieved using an interference filter centered at 265 nm, having a transmission efficiency at this wavelength of only 1.2%. Based on the level population estimate, and $M1$ branching ratios, only 5.7% of the stored ions contributed to this measurement. An unweighted double exponential fit to the data, including a constant background, resulted in a lifetime of $\tau(Fe\ XII, 3s^2 3p^3\ ^2P_{3/2}) = 1.85 \pm 0.24$ ms. The relatively large uncertainty in this measurement is a result of the weak signal strength and close proximity in time to the initial ion transient. The calculation by Mendoza and Zeippen, which lies 1.25 standard deviations from the measurement, is in worst agreement.

The $^2P_{1/2}$ level decays by an $M1$ transition, and at the 1% level an $E2$ (electric quadrupole) transition, to the $^2D_{3/2}$ level with a wavelength calculated to be near 307 nm. Although the $^2P_{3/2}$ population cascades into the $^2P_{1/2}$ level, the branching ratio is less than 0.1%, small enough to be ignored. The $^2D_{3/2}$-$^2P_{1/2}$ transition, which represents 29% of the total decay rate of the upper level, was observed experimentally using an interference filter centered at 308.8 nm. Fluorescence from 2.5×10^4 trapping cycles was collected. Since data beyond 7.3 decay constants seemed to decay more slowly than expected, the last 50 data points were discarded and a flat background was assumed. The remaining data, accounting for 99.9% of the level decay, were fitted with an unweighted double exponential plus a constant (see Fig. 4), resulting in a measured lifetime $\tau(Fe\ XII, 3s^2 3p^3\ ^2P_{1/2}) = 4.38 \pm 0.42$ ms. All theoretical calculations fall below this result, with the closest calculation falling within one standard deviation of the experimental error.

One $M1$ transition near 240 nm accounts for the decay of the $^2D_{3/2}$ level population estimated to start at around 20%. However, this decay may not have a single exponential de-
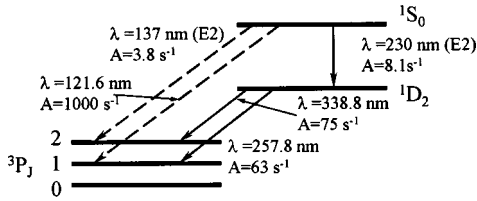
FIG. 5. The ground term level diagram for Fe XIII, showing the theoretical rates and wavelengths of the primary ($M1$) decay modes [11].

pendence, since all of the upper-level populations discussed above cascade into this level with non-negligible rates. The $^2D_{3/2}$ level population as a function of time $p_{3/2}(t)$ can be described using the following rate equation [12]:

$$p_{3/2}(t) = (0.404)\exp(-48.1t) - (0.073)\exp(-598.3t)$$
$$- (0.037)\exp(-245.1t) + (0.006)\exp(-2.7t). \tag{1}$$

The terms in this expression do not represent contributions from specific upper levels; rather they have been grouped mathematically. The first term corresponds to the decay of interest, while the second and third terms cause an initial rise in the model data. Fitting the model with a single exponential, after discarding the first few ms of data corresponding to roughly three time constants of the cascading $^2P_{1/2}$ level, produced a time constant within 1% of the decay time in the first term of Eq. (1).

An interference filter centered at 250 nm, having a bandwidth of 12 ± 2 nm, was used in this measurement because a 240-nm filter was not readily available. Since the $^2D_{3/2}$-$^2P_{3/2}$ transition discussed above was also within the passband, a double exponential was used to fit the fluorescence data. The shorter time constant initially generated by the fit matched the lifetime of the $^2P_{3/2}$ level, and was therefore fixed at $\tau_1=\tau(^2P_{3/2})$. The longer exponential decay was associated with the level lifetime $\tau($Fe XII, $3s^23p^3\ ^2D_{3/2})=20.35\pm1.24$ ms. The closest calculation is within one standard deviation of this measurement.

D. Fe XIII, $3s^23p^2\ ^1D_2$

The ground term levels of Fe XIII are shown in Fig. 5 along with the prominent $M1$ transitions. Measurement of the fast (1 ms) decay of the $^1S_0$ population was not feasible with this apparatus. However, the population of the $^1D_2$ level is not expected to be significantly increased by cascading from the upper $^1S_0$ level due to the small statistical population of this level, only 7%, and minimal weight of the $^1D_2$-$^1S_0$ branch. The $^1D_2$ level lifetime was measured by isolating the stronger of the two $M1$ transitions using an interference filter centered at 337 nm. After correcting for the ion storage time, a lifetime $\tau($Fe XIII, $3s^23p^2\ ^1D_2)=6.93\pm0.18$ ms was obtained.

Disparities between the tabulated decay rates for the $^1D_2$ level make this measurement particularly interesting. The

$M1$ decay rates to the $^2P_2$ and $^2P_1$ levels of 57.5 and 45.7 s^{-1}, tabulated by Kaufman and Sugar [13], result in a lifetime of 9.69 ms, 40% higher than measured. Despite citing the same reference, Huang's MCDF calculation [22], Fuhr, Martin, and Wiese [11] listed $M1$ rates of 75 and 63 s^{-1}, and when small ($<1\%$)$E2$ components are included a lifetime of 7.24 ms is obtained, differing from experiment by 4.5%. The present semiempirical calculation yields the same result as Ref. [11], which is the closest to the measurement. Eidelsberg, Crifo-Magnant, and Zeippen [15] cited even faster decay rates of 87 and 72 s^{-1}, leading to a lifetime of 6.29 ms, which is 9% faster than measured. Subsequently Mendoza and Zeippen [16] recalculated the decay rates, and their $M1$ rates were 84.7 and 70.1 s^{-1}, leading to a $^1D_2$ level lifetime of 6.45 ms, which is 7% shorter than the experimental value of 6.93 ± 0.18 ms.

E. Fe XIV, $3s^23p\ ^2P_{3/2}$

The level diagram and fluorescence data associated with the $^2P_{1/2}$-$^2P_{3/2}$ ''green line'' transition in Fe XIV were presented in Ref. [27]. Although a Fe^{13+} beam current of only 0.5 μA was obtained the large, 67%, statistical weight of the upper level benefited this measurement. The measured level lifetime $\tau($Fe XIV, $3s^23p\ ^2P_{3/2})=17.52\pm0.29$ ms. All calculations fall within 5% of this value, but the present calculation lies closest.

V. OVERVIEW

The theoretical transition rates contributing to a given level lifetime depend on two calculated parameters: the transition wavelength, or energy-level separation, and the matrix element. For $M1$ transitions, the matrix element depends on the angular parts of the wave function, while the energy levels depend more on the radial parts of the wave function. When wavelengths are measured, they can be used in place of the calculated wavelengths to potentially improve the accuracy of the transition rate calculations. For the Fe ions studied here, the relevant decay wavelengths have all been determined experimentally, except for several transitions associated with the ^2P levels in P-like Fe XII [11]. Thus the matrix element calculations can be tested using the present Fe experimental data.

It is now also possible to compare the theory against experimental data for neighboring charge states of both Fe and Mn ions. Figure 6(a) shows the percent difference between data from three theoretical compilations for Fe ions and the experimental lifetimes, with the zero value representing the experimental data. The isoelectronic sequences are identified at the bottom of the plot. Data from the tabulations by Fuhr, Martin, and Wiese [11,28] with the S-like data points supplemented from Chou $et\ al.$ [20] representing multiconfiguration Hartree-Fock (MCHF) calculations, are marked with circles; Thomas-Fermi type calculations by Mendoza and Zeippen [16–18] are indicated by squares, while x's are used to represent the compilation of older data by Eidelsberg,
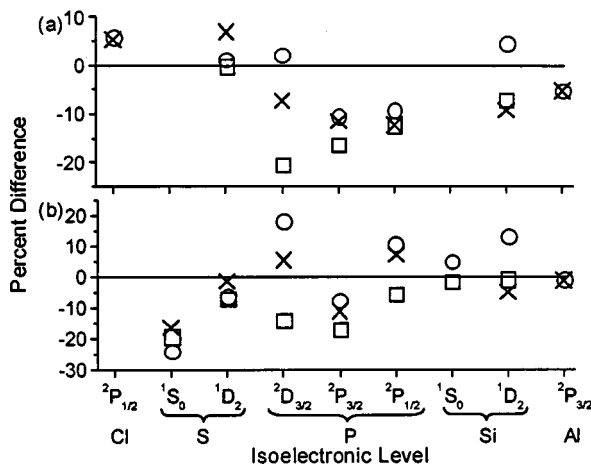
FIG. 6. The percent difference between three theoretical data sets and the experiment level lifetimes, with the zero value representing the experimental data. (a) The Fe ion experimental data described in this paper compared with theoretical lifetimes. (b) The Mn ion experimental data from Ref. [12] compared to theoretical lifetimes. Data from Fuhr, Martin and Wiese [11,28], and Chou *et al.* [20], representing MCHF calculations, are indicated by circles. Thomas-Fermi type calculations by Mendoza and Zeippen [16–18] are indicated with squares, while ×'s are used to represent the compilation of Eidelsberg, Crifo-Magnant, and Zeippen [15].

Crifo-Magnant, and Zeippen [15]. Figure 6(b) is based on the experimental Mn ion lifetime data from Ref. [12]. With few experimental wavelengths available [13], the theoretical transition rates used to determine the Mn level lifetimes associated with this plot must be based upon calculated wavelengths. The theory is presented in the same way as in Fig. 6(a).

One can see in Fig. 6 that no substantial improvements in lifetime accuracy have emerged from the use of different theoretical techniques, although the MCHF lifetimes may have marginally better agreement with experiment. There is also no significant difference in the agreement between theory and experiment for Fe and Ma. Larger differences are associated with the stages of ionization. The calculations for the ^2P and ^2D levels of the P-like ions (five electrons outside a closed shell) exhibit the largest disagreements with experiment, although the ^1S level of S-like Mn (four electrons outside a closed shell) also shows a large disparity. The Thomas-Fermi calculations [16–18] tend to fall below the experimental results, although the calculations for the Si-like Mn ion lifetimes and that of the ^1D level of S-like Fe are quite accurate. A rather smooth trend of the older calculated values from the Eidelsberg compilation for the Fe lifetimes can be noted, but this is less apparent in the Mn data.

The present *ab initio* transition rate calculations in Table I typically do not improve on the (selected) ''best'' rates from the earlier calculations, i.e., those rates which result in lifetimes closest to the present data, except for the case of Fe XIV. When the present calculations are converted to semiempirical calculations by the substitution of experimental energy-level separations, then improved agreement with experiment is obtained for all measurements (for which calculations were made) except for Fe XIV. One may conclude from this, and from the information presented above, that theoretical energy-level separations are still a contributing factor in theoretical accuracy for these configurations. The semiempirical lifetimes lie between two and approximately three standard deviations of the experimental uncertainty from the data. These deviations must be associated with the matrix elements. The use of experimental energy separations decreases the calculated lifetimes for Fe X, Fe XI, and Fe XIV, but increases the calculated lifetimes for Fe XII and Fe XIII. The semiempirical lifetimes are longer than the experimental lifetimes in all cases but Fe XIV.

It is also possible to compare the ratios of the experimental lifetimes for the same configurations in Mn and Fe. The most precise comparisons are obtained for the $3s^2 3p^4 \, ^1D_2$ level of Mn X–Fe XI and the $3s^2 3p^2 \, ^1D_2$ level of Mn XII–Fe XIII. These measured lifetime ratios are respectively 1.83 ± 0.03 and 1.61 ± 0.035. Less precise lifetime ratios were obtained for other configurations and levels, with most values lying between these higher precision results. The differences in the ratios are thought to be associated with different relative polarizabilities of the electronic shells of each configuration.

VI. CONCLUSION

Astrophysical and theoretical importance can be ascribed to the atomic data presented in this paper. Seven level lifetimes in five charge states of Fe ions were measured utilizing confined ions extracted from an ECR ion source. In addition, the previously unobserved $^2D_{3/2}$-$^2P_{1/2}$ transition in Fe XII was observed in the laboratory, although the wavelength was only obtained within the bandwidth of an interference filter. Transition rates for the well-known ''red'' and ''green'' lines in Fe X and Fe XIX were measured to better than 2% in a few hours of data collection time. In general, the theoretical level lifetimes from previously untested transition rate calculations differ from experiment by less than 12%, with some calculations happening to be in excellent agreement with experiment. Many of the measurements provide a clear test of the theory. Based on calculations presented here, it now appears that the energy-level calculations are a contributing factor in the accuracy of many *ab initio* transition rate calculations, but calculations of magnetic dipole transition matrix elements still account for the main differences between experiment and theory.

ACKNOWLEDGMENTS

[1] J. P. Lynch and M. Kafatos, Astrophys. J., Suppl. **76**, 1169 (1991).

[2] D. A. Church, Phys. Rep. **228**, 253 (1993).

[3] M. H. Prior and H. A. Shugart, Phys. Rev. Lett. **27**, 902 (1971).

[4] L. Yang and D. A. Church, Phys. Rev. Lett. **70**, 3860 (1993).

[5] B. J. Wargelin, P. Beiersdorfer, and S. M. Kahn, Phys. Rev. Lett. **71**, 2196 (1993).

[6] J. Doerfert, E. Traebert, and A. Wolf, Hyperfine Interact. **99**, 155 (1996).

[7] J. Arianer and R. Geller, Annu. Rev. Nucl. Part. Sci. **31**, 19 (1981).

[8] L. Yang and D. A. Church, Nucl. Instrum. Methods Phys. Res. B **56/57**, 1185 (1991).

[9] D. P. Moehs, D. A. Church, and R. Phaneuf, Rev. Sci. Instrum. **69**, 1991 (1998).

[10] B. R. Beck, J. Steiger, G. Weinberg, D. A. Church, J. Mc-Donald, and D. Schneider, Phys. Rev. Lett. **77**, 1735 (1996).

[11] J. R. Fuhr, G. A. Martin, and W. L. Wiese, J. Phys. Chem. Ref. Data Suppl. **17**, 4 (1998).

[12] D. P. Moehs and D. A. Church, Phys. Rev. A **59**, 1884 (1999).

[13] V. Kaufman and J. Sugar, J. Phys. Chem. Ref. Data **15**, 321 (1986).

[14] W. R. Johnson, M. Idrees, and J. Sapirstein, Phys. Rev. A **35**, 3218 (1986); W. R. Johnson and J. Sapirstein, Phys. Lett. **57**, 1126 (1986).

[15] M. Eidelsberg, F. Crifo-Magnant, and C. J. Zeippen, Astron. Astrophys., Suppl. Ser. **43**, 455 (1981).

[16] C. Mendoza and C. J. Zeippen, Mon. Not. R. Astron. Soc. **199**, 1025 (1982).

[17] C. Mendoza and C. J. Zeippen, Mon. Not. R. Astron. Soc. **198**, 127 (1982).

[18] C. Mendoza and C. J. Zeippen, Mon. Not. R. Astron. Soc. **202**, 981 (1983).

[19] K.-N. Huang, Y.-K. Kim, K. T. Cheng, and J. P. Desclaux, At. Data Nucl. Data Tables **28**, 355 (1983).

[20] H.-S. Chou, J.-Y. Chang, Y.-H. Chang, and K.-N. Huang, At. Data Nucl. Data Tables **62**, 77 (1996).

[21] K.-N. Huang, At. Data Nucl. Data Tables **30**, 313 (1984).

[22] K.-N. Huang, At. Data Nucl. Data Tables **32**, 503 (1985).

[23] K.-N. Huang, At. Data Nucl. Data Tables **34**, 1 (1986).

[24] A. K. Bhatia and G. A. Doschek, At. Data Nucl. Data Tables **60**, 97 (1995).

[25] A. K. Bhatia and G. A. Doschek, At. Data Nucl. Data Tables **64**, 183 (1996).

[26] D. P. Moehs, D. A. Church, M. I. Bhatti, and W. F. Perger, Phys. Rev. Lett. **85**, 38 (2000).

[27] D. P. Moehs and D. A. Church, Astrophys. J. **516**, L111 (1999).

[28] G. A. Martin, J. R. Fuhr, and W. L. Wiese, J. Phys. Chem. Ref. Data Suppl. **17**, 3 (1998).